Size-Reduced Equilateral Triangular Metamaterial Patch Antenna Designed for Mobile Communications

Guoxiang Dai [1], Xiaofei Xu [1,2,*], and Xiao Deng [1]

[1] School of Communication and Information Engineering
Shanghai University, Shanghai, 200444, China

[2] Key Laboratory of Specialty Fiber Optics and Optical Access Networks
Shanghai Institute for Advanced Communication and Data Science
Shanghai University, Shanghai 200444, China
*xfxu@shu.edu.cn

Abstract ─ A size-reduced equilateral triangular metamaterial patch antenna (ETMPA) is proposed for the 5G mobile communications. The new ETMPA is formed from a conventional equilateral triangular patch antenna (ETPA) by additionally loading triangular-shaped mushroom metamaterials. One ETMPA is experimentally demonstrated. It is shown to resonate at 3.488GHz. The side length is only $0.483\lambda_g$, which is much smaller than that for a conventional ETPA with a length of $0.66\lambda_g$. Despite its compactness, the ETMPA has an acceptable bandwidth of 2.1% and antenna gain of 6.3dBi in measurement. These performances make the compact ETMPA proposing to be used in the wireless communications at 3.5GHz.

Index Terms ─ Equilateral triangular patch antenna, metamaterials, size-reduced.

I. INTRODUCTION

With the rapid development of mobile wireless communications, there have been increasing demands for compact patch antennas. Among various choices of different patch shapes, it is interesting to note that an equilateral triangle patch antenna (ETPA) [1-6] has a relatively smaller patch than its square and circular counterparts, although the latter two kinds of antennas are better known [1]. The side length of ETPA is about $0.66\lambda_g$ (λ_g is the guided wavelength of substrate at the resonant frequency) [1], assuming it works at the lowest fundamental mode. The associated patch area is nearly $0.19\lambda_g^2$. However for a square patch antenna, the side length is nearly $0.5\lambda_g$ [1] while patch area is about $0.25\lambda_g^2$. The case for the circular patch antenna is similar. The diameter for the circular patch is about $0.58\lambda_g$. The patch area is as large as $0.26\lambda_g^2$ [1]. Both of them are assumed to operate at their fundamental modes respectively.

To further compact the ETPA for the potential 5G mobile communications, a new approach is proposed in this work by employing the metamaterial technology [7-14]. Metamaterials are man-made subwavelength structures that exhibit an effective permittivity or permeability, and thus equivalent to some natural materials. Inspired by the square-shaped mushroom metamaterials designed for a compact rectangular patch antenna [14], triangle-shaped mushroom metamaterials (TSMMs) are used in this contribution to adapt for an ETPA. A new equilateral triangle metamaterial patch antenna (ETMPA) is hence formed by filling the TSMMs into a conventional ETPA. The TSMMs are physically made from low permittivity substrates, but work as some effective materials with an enhanced high dielectric constant, similar with their square-shaped equivalents [14].

A practical ETMPA is designed to operate at 3.5GHz. The antenna characteristics are studied in both numerical simulations and experiments. Results are observed in good agreement. The practical ETMPA has a side length of 24mm. However it resonates at 3.488GHz in experiments. Considering the TSMMs are made from substrates with low dielectric constant of 3, the electrical length for the ETMPA is only $0.483\lambda_g$, by normalizing 24mm to the λ_g (49.67mm) at 3.488GHz. The patch area is about $0.1\lambda_g^2$, which is much smaller than that for a conventional ETPA. The new ETMPA has a -10dB bandwidth of 73MHz (2.1%), ranging from 3.451 to 3.524GHz in measurement. The peak measured antenna gain is 6.3dBi. Within the working bandwidth, the antenna gain is observed not less than 5.8dBi. Considering the compact patch size, the bandwidth and antenna gain for the ETMPA are however not much sacrificed. Both are acceptable that make the new antenna promising in the applications of 5G mobile communication at the 3.5GHz band.

Submitted On: June 20, 2021
Accepted On: July 21, 2021

https://doi.org/10.47037/2021.ACES.J.360811

II. ANTENNA DESIGN

The configuration of the proposed compact ETMPA is shown in Fig. 1. It is shown with numerous metallic triangle-shaped mushroom structures embedded in the substrate. These triangle-shaped structures are designed to fit for the configuration of an ETPA. The substrate of ETMPA is divided into two sub-layers by the mushroom structures. The upper layer is assumed with thickness h_1, dielectric constant ε_{r1}, and loss tangent $tan\delta_1$, while the lower layer is with h_2, ε_{r2}, and $tan\delta_2$. Both can be made from low index laminates that are commonly found. The mushroom structures are designed in the lower substrate layer. Each mushroom element has a small triangle cap mounted on the top of lower substrate, which is connected to the ground plane by a conducting via located in the center of element. A total number of m^2 (m is an integer) triangle-shaped mushroom elements are included beneath the patch. In Fig. 1, an example of m = 4 is shown. Considering that the ETMPA is with a side length of L, and the side length for the mushroom element is p, we have $L = m \times p$. The triangle mushroom cap is assumed with side length of a, which is very close to (but still less than) p. The outer diameter for the perforated vias is d. The length for the ground plane is G. The antenna is fed by a 50Ω coaxial probe. In order to prevent the inner pin of probe from overlapping those metallic mushrooms, two mushroom elements around the feeding position are designed defected by removing the conducting vias.

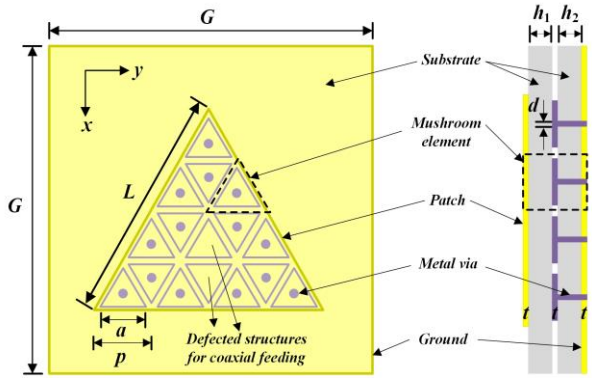

Fig. 1. Configuration of the ETMPA.

These mushroom structures can be regarded as effective metamaterials if p is much smaller than wavelength [7-8]. The effective permittivity ε_{reff} is irrelevant to the shapes of the structure since it originates from the enhanced capacitive effect in the substrate [14]. The underlying mechanism is much different from the electromagnetic bandgap or high impedance surface applications in [15-18], in which the period p is generally at the order of 0.25 to 0.5 wavelength. For the composite TSMMs, the ε_{reff} is approximate to that for those rectangular-shaped mushroom metamaterials [14] as:

$$\varepsilon_{reff} \approx \varepsilon_{r1} \frac{h_1 + h_2}{h_1}. \quad (1)$$

The resonant frequency f_0 of fundamental TM_{10} mode can be hence estimated [1-6] using:

$$f_0 \approx \frac{2c}{3L\sqrt{\varepsilon_{reff}}} \approx \frac{2c}{3L\sqrt{\varepsilon_{r1}}} \sqrt{\frac{h_1}{h_1 + h_2}}, \quad (2)$$

where c is the light speed in free space.

The side length L for the ETMPA normalized to λ_g is:

$$\frac{L}{\lambda_g} \approx \frac{2}{3} \sqrt{\frac{h_1}{h_1 + h_2}}, \quad (3)$$

in which an additional reduction ratio $\sqrt{h_1/(h_1+h_2)}$ is included. It makes the electrical length of the ETMPA much reduced than the conventional. The principles introduced above provide good starting points to design a compact ETMPA.

III. RESULTS

One practical ETMPA is designed operating at 3.5GHz for the 5G mobile communications in the Sub-6GHz band [19-20]. It is first optimized in the full wave solver Ansys HFSS. An optimal set of parameters are obtained as following: L = 24 mm, G = 50 mm, p = 6 mm, a = 5.4 mm, $h_1 = h_2$ = 1.52mm, and d = 1mm.

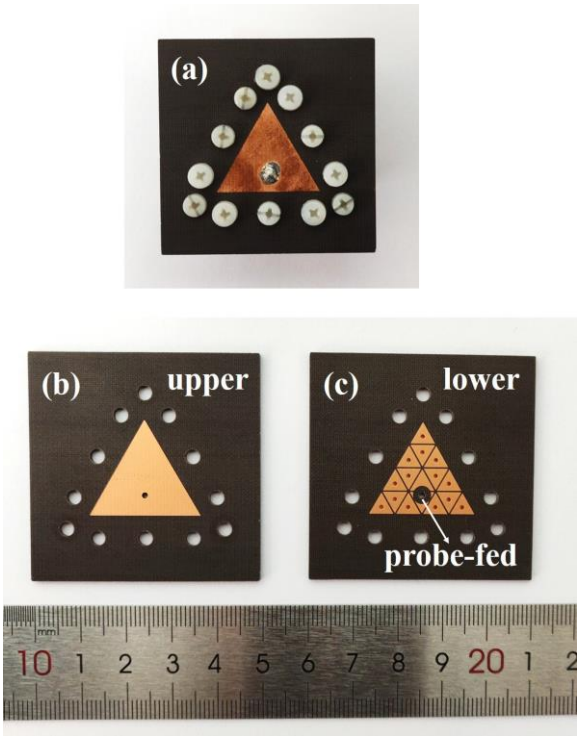

Fig. 2. The photograph for (a) the assembled ETMPA, (b) the upper layer, and (c) the lower layer.

The dielectrics for the two sub-layers to support the TSMMs are both chosen to be the SCGA-500 GF300 provided by Shengyi Technology Co. Ltd. (SYTECH), with $\varepsilon_{r1} = \varepsilon_{r2} = 3$, and $tan\delta_1 = tan\delta_2 = 0.0023$.

An antenna sample is further manufactured for the experimental demonstration using these optimal parameters. It is manually assembled from two substrate layers which are fabricated independently, with the help of nylon screws. The assembled ETMPA is shown in Fig. 2 (a). The upper layer is given in Fig. 2 (b) showing the equilateral triangle patch. The lower layer is shown in Fig. 2 (c). The triangle mushroom caps of the TSMMs are seen on the substrate. The ETMPA is fed by a coaxial probe. Two mushroom elements near the feeding point are defected without vias.

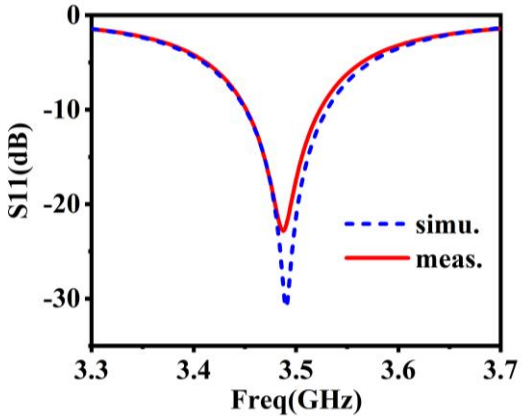

Fig. 3. The reflection coefficients of the ETMPA.

The simulated and measured reflection coefficients (S11s) for the proposed ETMPA is given in Fig. 3. They are seen in good agreement. It is revealed from the measured results that the antenna resonates at 3.488GHz. This value is close to 3.4GHz that is predicted from equation (2). The measured -10dB bandwidth for the ETMPA is 73MHz (2.1%) ranging from 3.451 to 3.524GHz. The simulated bandwidth is slightly wider as 79MHz from 3.451 to 3.53GHz.

It is interesting to notice that the electrical length for the practical ETMPA is now $0.483\lambda_g$, by normalizing the physical length 24mm to the λ_g (49.67mm) at 3.488GHz. This result agrees well with the theoretical prediction of about $0.47\lambda_g$ according to equation (3). The patch area is calculated to be only about $0.1\lambda_g^2$. However according to [1-6], the side length for a conventional ETPA is at the order of $0.66\lambda_g$, while the patch area is nearly $0.19\lambda_g^2$. These results convincingly prove that the new ETMPA has a much reduced patch area than the conventional ETPA. The size reduction effect is mainly influenced by the thickness ratio of h_1 and h_2. By further increasing the ratio of h_2 over h_1, the ETMPA can be designed even smaller in future. If we alternatively use the free space wavelength λ_0 (86mm) at 3.488GHz to measure the ETMPA, the new antenna now occupies a patch area of $0.034\lambda_0^2$. The total thickness is $0.035\lambda_0$ by normalizing 3.04mm to 86mm.

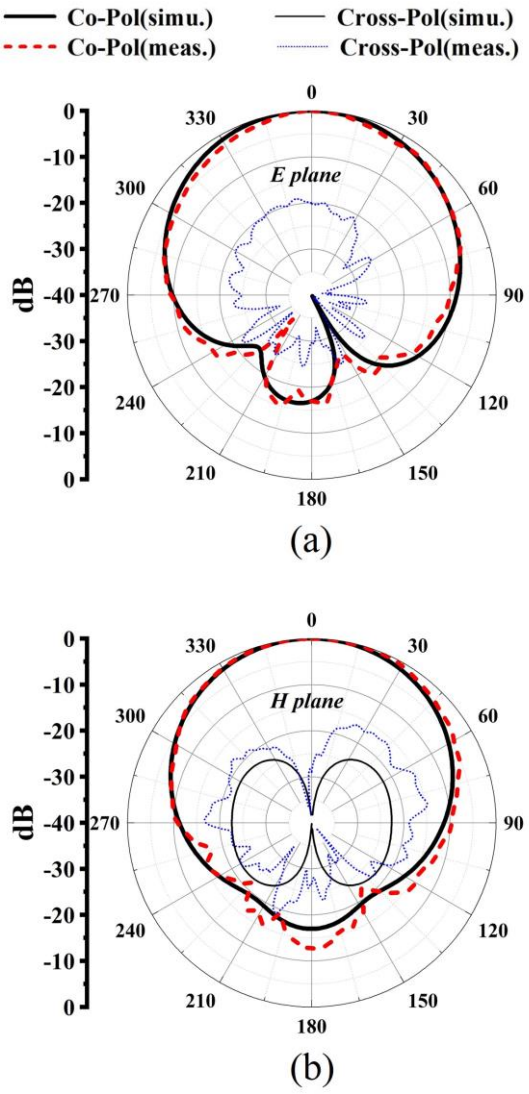

Fig. 4. The radiation patterns for the ETMPA at 3.5GHz on the (a) E plane and (b) H plane.

The radiation patterns for the ETMPA at 3.5GHz are also studied and given in Fig. 4. The patterns on the E plane (*xoz* plane) and H plane (*yoz* plane) are shown in Fig. 4 (a) and Fig. 4 (b), respectively. It is observed that the simulated and measured co-polarized patterns are almost the same. The front-to-back ratio is at the order of 15dB. The cross-polarization levels are however different on the E and H planes. The simulated cross-polarized levels are below -40dB on the E plane that are almost unseen, and about -22dB on the H plane. The measured cross-polarizations are nevertheless much

higher, which are seen to be -18.8dB on the E plane, and -14.6dB on the latter H plane.

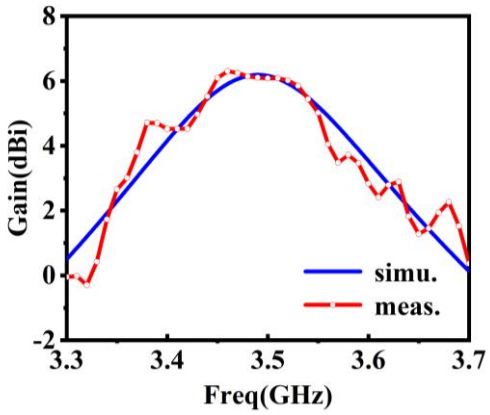

Fig. 5. The antenna gain.

The antenna gain curves are given in Fig. 5 obtained from numerical predictions and experiments. Their trends versus frequency are similar. The peak (realized) antenna gain predicted from HFSS is 6.2dBi. For the measured (realized) gain, the peak value is 6.3dBi. Within the operating frequency band, the measured antenna gain is all over 5.8dBi. The total (realized) efficiency of the fabricated ETMPA is not measured here. However, it is predicted to be about 91% from HFSS. Considering the similarities between the simulated and measured radiation patterns as shown in Fig. 4, the directivity for the fabricated ETMPA should be very close to that of the antenna model used in simulations. Hence the total efficiency for the practical ETMPA can be reasonably estimated at the level of 90%, according to the simulated value.

Table 1: Performances of several compact metamaterial antennas operating near 3.5GHz

Ref.	f_0 /GHz	Patch area	Thick-ness	BW /%	Gain /dBi
[11]	3.3	$0.036\lambda_0^2$	$0.034\lambda_0$	3.1	0.79
[12]	3.494	$0.063\lambda_0^2$	$0.087\lambda_0$	2.2	7
[13]	3.5	$0.053\lambda_0^2$	$0.018\lambda_0$	3.7	4.6
This	3.488	$0.034\lambda_0^2$	$0.035\lambda_0$	2.1	6.3

The antenna performances are shown in Table 1, in contrast to several other compact metamaterial antennas [11-13] operating near 3.5GHz. In Table 1, all of the patch areas and thicknesses are normalized to the free space wavelength λ_0 at the resonant frequency f_0. In the BW column, results are summarized from the -10dB relative bandwidth of these antennas. From Table 1, the ETMPA is observed to occupy a very compact antenna volume but maintain an acceptable bandwidth and gain. To further improve the bandwidth, several broadband techniques [1], e.g., adding a stacked patch, or using a U-slot patch etc., might be used in future.

IV. CONCLUSION

A new compact ETMPA is designed and realized operating at 3.5GHz. By loading periodic TSMMs into a conventional ETPA, the new ETMPA is demonstrated with a reduced patch area than conventional. Moreover, the bandwidth and radiation performances for the size-reduced ETMPA are also evaluated. The measured bandwidth for the practical compact ETMPA is 2.1% while the peak antenna gain is about 6.3dBi. They are both sufficient to meet the demand of 5G mobile communications.

ACKNOWLEDGMENT

This work is supported by the National Natural Science Foundation of China (No. 11904222) and the Natural Science Foundation of Shanghai (No. 16ZR1446100).

REFERENCES

[1] R. Garg, P. Bhartia, I. Bahl, and A. Ittipiboon, *Microstrip Antenna Design Handbook*. Artech House, USA, 2001.

[2] J. Helszajn and D. S. James, "Planar triangular resonators with magnetic walls," *IEEE Trans. Microw. Theory Techn.*, vol. 26, pp. 95-100, 1978.

[3] E. F. Kuester and D. C. Chang, "A geometrical theory for the resonant frequencies and Q-factors of some triangular microstrip patch antennas," *IEEE Trans. Antennas Propag.*, vol. 31, pp. 27-34, 1983.

[4] K.-F. Lee, K. Luk, and J. S. Dahele, "Characteristics of the equilateral triangular patch antenna," *IEEE Trans. Antennas Propag.*, vol. 36, pp. 1510-1518, 1988.

[5] N. Kumprasert and K. W. Kiranon, "Simple and accurate formula for the resonant frequency of the equilateral triangular microstrip patch antenna," *IEEE Trans. Antennas Propagat.*, vol. 42, pp. 1178-1179, 1994.

[6] M. Biswas and M. Dam, "Fast and accurate model of equilateral triangular patch antennas with and without suspended substrates," *Microw. Opt. Techn. Lett.*, vol. 54, pp. 2663-2668, 2012.

[7] J. B. Pendry, A. J. Holden, D. J. Robbins, and W. J. Stewart, "Magnetism from conductors and enhanced nonlinear phenomena," *IEEE Trans. Microw. Theory Techn.*, vol. 47, pp. 2075-2084, 1999.

[8] C. Caloz and T. Itoh, *Electromagnetic Metamaterials: Transmission Line Theory and Microwave Applications*. Wiley, USA, 2005.

[9] Y. Dong and T. Itoh, "Metamaterial-based antennas," *Proc. IEEE*, vol. 100, pp. 2271-2285,

2012.

[10] J. Wang, Y. Li, Z. H. Jiang, T. Shi, M.-C. Tang, Z. Zhou, Z. N. Chen, and C.-W. Qiu, "Metantenna: when metasurface meets antenna again," *IEEE Trans. Antennas Propag*., vol. 68, pp. 1332-1347, 2020.

[11] J. Zhu and G. V. Eleftheriades, "A compact transmission-line metamaterial antenna with extended bandwidth," *IEEE Antennas Wireless Propag. Lett*., vol. 8, pp. 295-298, 2009.

[12] X. M. Yang, Q. H. Su, Y. Jing, Q. Cheng, X. Y. Zhou, H. W. Kong, and T. J. Cui, "Increasing the bandwidth of microstrip patch antenna by loading compact artificial magneto-dielectrics," *IEEE Trans. Antennas Propag*., vol. 50, pp. 373-378, 2011.

[13] T. Cai, G. M. Wang, X. F. Zhang, Y. W. Wang, B. F. Zong, and H. X. Xu, "Compact microstrip antenna with enhanced bandwidth by loading magneto-electro-dielectric planar waveguided metamaterials," *IEEE Trans. Antennas Propag.*, vol. 63, pp. 2306-2311, 2015.

[14] X. Xu and J. Wei, "Miniaturisation design of patch antenna using a low-profile mushroom type meta-substrate tailored with high permittivity," *IET Microw. Antennas Propag.*, vol. 12, pp. 1216-1221, 2018.

[15] D. Sevenpiper, L. Zhang, R. F. Broas, and N. G. Alexopolous, "High-Impedance electromagnetic surfaces with a forbidden frequency band," *IEEE Trans. Microw. Theory Techn*., vol. 47, pp. 2059-2074, 1999.

[16] L. Li, Q. Chen, Q. Yuan, C. Liang, and K. Sawaya, "Surface-wave suppression band gap and plane-wave reflection phase band of mushroomlike photonic band gap structures," *J. Appl. Phys*., vol. 103, p. 023513, 2008.

[17] T. Jiang, T. Jiao, and Y. Li, "Array mutual coupling reduction using L-loading E-shaped electromagnetic band gap structures," *Int. J. Antennas Propag.*, 2016, 6731014, 2016.

[18] T. Jiang, T. Jiao, and Y. Li, "A low mutual coupling MIMO antenna using periodic multi-layered electromagnetic band gap structures," *Applied Computational Electromagnetics Society Journal*, vol. 33, pp. 305-311, 2018.

[19] WRC-15 Press Release. (Nov. 27, 2015). World Radio communication Conference Allocates Spectrum for Future Innovation. Online website: http://www.itu.int/net/pressoffice/press_releases/2015/56.aspx

[20] Z. Li, J. Han, Y. Mu, X. Gao, and L. Li, "Dual-band dual-polarized base station antenna with a notch band for 2/3/4/5G communication systems," *IEEE Antennas Wireless Propag. Lett*., vol. 19, pp. 2462-2466, 2020.